SCIENCE CHINA
Information Sciences

• RESEARCH PAPER •

March 2026, Vol. 69, Iss. 3, 132303:1–132303:18
https://doi.org/10.1007/s11432-025-4672-1

Efficient adaptive random network coding for video content dissemination in NR-V2X networks

Junchao MA[1*], Bodong SHANG[2], Yang YU[1] & Pingzhi FAN[3]

[1]*School of Electrical and Information Engineering, Jiangsu University of Technology, Changzhou 213001, China*
[2]*Zhejiang Key Laboratory of Industrial Intelligence and Digital Twin, Eastern Institute of Technology, Ningbo 315200, China*
[3]*School of Information Science and Technology, Southwest Jiaotong University, Chengdu 611756, China*

Received 22 April 2025/Revised 15 September 2025/Accepted 7 November 2025/Published online 20 January 2026

Abstract High-bandwidth content, particularly video and video-like data, has become increasingly common in recent vehicular networks. This encompasses everything from real-time high-resolution maps and sensor data shares to vehicle overtaking videos and infotainment streams. However, due to the high mobility of vehicles and the large volume of video data, roadside units encounter challenges in efficiently disseminating specific video content to multiple vehicles within strict deadlines. To address this issue, we propose the use of adaptive random network coding (ARNC) for multicasting video content in new radio (NR) vehicle-to-everything (V2X) networks to maximize the quality received by target vehicles. However, ARNC requires frequent feedback from vehicles via the physical sidelink feedback channel, resulting in significant overhead in NR V2X networks. To strike a balance between video quality and feedback costs, we introduce a partial feedback ARNC (PARNC)-based scheduling scheme and establish a utility function to evaluate its performance. We also employ a deep reinforcement learning algorithm to optimize the PARNC design, thereby achieving a locally optimal solution. Extensive simulations validate the PARNC performance against other benchmarks. The results show that PARNC outperforms alternative schemes, particularly when the utility function emphasizes transmission performance and when feedback costs are manageable.

Keywords new radio vehicle-to-everything, video content dissemination, adaptive random network coding, deep reinforcement learning

Citation Ma J C, Shang B D, Yu Y, et al. Efficient adaptive random network coding for video content dissemination in NR-V2X networks. Sci China Inf Sci, 2026, 69(3): 132303, https://doi.org/10.1007/s11432-025-4672-1

1 Introduction

As the development of the Internet of Vehicles (IoV) accelerates, an increasing number of vehicles are becoming interconnected, forming a complex network that is indispensable for advanced traffic management and autonomous driving [1,2]. However, there are several challenges, such as decreased driving efficiency and elevated accident rates. From a communication perspective, ensuring highly reliable and low-latency distribution of traffic data to vehicles is crucial for safe and efficient driving [3]. Numerous IoV applications heavily rely on video data or video-like data to facilitate real-time decision-making, including real-time traffic monitoring, collision avoidance systems, lane-keeping assistance, and 3D point cloud high-definition maps [4–6].

The increasing demand for video data in IoV applications highlights the need for efficient communication frameworks to distribute video data [7, 8]. Unlike conventional data types, video data require high bandwidth, low latency, and robust connectivity in time-sensitive scenarios. The main challenges in video data transmission within IoV systems stem from two key factors: the large data volume of video content and the high mobility of connected vehicles [9–11]. Video files are inherently data-intensive and consume significant network resources, necessitating an efficient source encoding method [12–14]. Furthermore, vehicles travel at high speeds and traverse varying network conditions, making it critical to maintain stable communication links and leverage advanced scheduling schemes for video data distribution [15–18]. The efficient distribution of video data in vehicular networks has attracted significant attention in both academic and industrial circles.

To address these issues, extensive research has been conducted across the physical and network layers [19–21]. Among the myriad of potential techniques, network coding (NC) is a promising approach to improving transmission efficiency [22–25]. The essence of NC involves multiplexing content chunks together in the transmission. Instead of requiring the target vehicle to receive every chunk of the requested content exactly, the original data can be recovered

* Corresponding author (email: junchao_ma@foxmailcom)

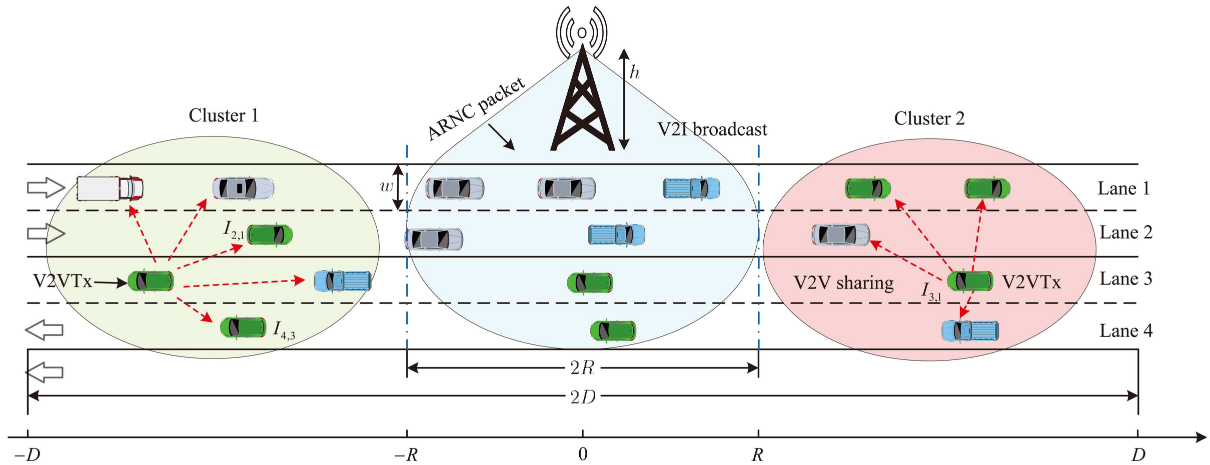

Figure 1 (Color online) Applied system model of the cooperative V2I and V2V communication for video dissemination.

as long as a predefined number of NC codes are received. Therefore, the negative impact of intermittent links and dynamic network topologies can be mitigated by receiving order-independent NC codes, rather than ensuring the successful reception of each individual content chunk. To date, previous studies have presented various NC techniques, such as random linear network coding (RLNC) [22], batched-sparse (BATS) coding [24], and adaptive random linear network coding (ARNC) [26]. In Section 2, we will briefly review these NC technologies, and readers can refer to the corresponding references for details and application scenarios. Among all NC technologies, ARNC achieves superior performance in numerous scenarios to enhance transmission efficiency. However, it requires frequent feedback from the receivers to the transmitter, indicating whether the transmission was successful in the ARNC design [27]. Depending on the latest 3GPP Release 17 and 18 standardizations, the feedback is sent in the physical sidelink feedback channel (PSFCH) to improve the reliability of the sidelink (SL) in the new radio (NR) vehicle-to-everything (NR V2X) networks [1]. However, PSFCH shares scarce time-frequency resources with the physical sidelink shared channel (PSSCH). Although each feedback message (e.g., an ACK/NACK) is small, the cumulative overhead from frequent feedback transmissions across a large vehicle population becomes significant. This consumption of limited radio resources diminishes the available capacity for data transmission, thereby reducing the overall system throughput. Consequently, frequent feedback poses a critical bottleneck in dense vehicular networks with high-volume video traffic. This challenge motivated the design of a feedback-efficient NC scheme in this study.

In this paper, we propose a reconstruction of the conventional ARNC scheme to better facilitate video data dissemination in NR V2X communications using SL transmission [4,8]. This revised scheme is called partial feedback ARNC (PARNC). Unlike traditional ARNC, which requires feedback from every receiver in each transmission, PARNC only requires feedback in specific transmissions. As shown in Figure 1, we consider a scenario where a roadside unit (RSU) needs to disseminate sensed video content, such as an HD map, to passing vehicles through vehicle-to-infrastructure (V2I) groupcast transmissions. However, some vehicles may be obstructed from the RSU due to vehicle mobility and obstacles, resulting in failed or suboptimal V2I transmission. In such instances, vehicles can relay disseminated data to nearby vehicles via vehicle-to-vehicle (V2V) transmission.

From a content perspective, we employ scalable video coding (SVC) to process the video data for dissemination. SVC encodes the video into multiple layers, including one base layer (BL) and several enhancement layers (ELs) [14]. BL contains the essential video information and can be decoded independently for basic video quality, whereas ELs progressively enhance the recovered video quality. In practice, the BL data are often provided with more protection and resources than the EL data during transmission because the BL data are more important than the EL data in the video decoding. This approach is called unequal error protection (UEP). By meticulously designing the ARNC and SVC schemes, vehicles with poor channel conditions can recover lower-quality video, and those with good channel conditions can retrieve high-quality video during the same multicast process [28]. This feature renders SVC ideal for data dissemination in diverse and time-varying channel conditions. Based on the SVC and PARNC, we propose a PARNC-based scheduling scheme which involves the PARNC construction and network resource allocation. A utility function is established to evaluate the scheduling scheme, measuring the balance between the quality of the received video and feedback cost. Additionally, an optimization problem is formulated to maximize the utility function through careful PARNC design, and a deep reinforcement learning (DRL) algorithm is used to solve the optimization problem. Extensive simulations are conducted to validate the proposed PARNC and compare the performance of different schemes across various parameter settings. The results show the superiority of the proposed approach, especially when the network priorities received video quality in the utility performance.

The main contributions of this paper are summarized as follows.

• First, this paper investigates cooperative V2V and V2I communication for video data dissemination. To quantify the tradeoff between received video quality and the signaling overhead incurred by feedback, a novel utility function is proposed. This model captures the opportunity cost of feedback, which is often overlooked in content dissemination design.

• Second, a novel PARNC-based scheduling scheme is proposed to balance the received video quality and incurred feedback cost. Unlike traditional full-feedback or no-feedback schemes, PARNC operates in a hybrid mode. It employs a blind, predefined transmission phase with zero feedback overhead to disseminate the most important video layers, followed by an adaptive feedback-driven phase to efficiently refine the transmission for enhanced layers. This represents a new point in the design space for adaptive NC. Additionally, a DRL algorithm is employed to determine the local optimal PARNC design by maximizing the formulated utility function.

• Finally, comprehensive simulations are conducted to validate the effectiveness of the proposed PARNC-based scheduling scheme under various network conditions. Comparisons with benchmark schemes are also performed. The results highlight the superiority of the PARNC-based scheduling scheme, particularly in scenarios where feedback cost significantly impacts the utility performance. These findings reveal that when feedback cost dominates, the optimal PARNC strategy involves transmitting predefined packets in each time slot to minimize unnecessary feedback.

The remainder of this paper is organized as follows. Section 2 reviews related work on data dissemination in vehicular networks. Section 3 introduces the system model and elaborates on the proposed scheduling scheme. In Section 4, we define a utility function to evaluate content dissemination performance and formulate a utility maximization problem. A DRL algorithm is then presented to solve this problem, enabling the derivation of a near-optimal scheduling scheme. Section 5 presents the simulation results validating the proposed scheme's performance and comparing it with benchmark approaches. Finally, Section 6 concludes this paper.

2 Literature review

In this section, we aim to provide a comprehensive literature review on cooperative V2V and V2I communication, as well as network coding assisted transmission. Additionally, we outline the motivation derived from prior research in these areas.

2.1 Cooperative V2V and V2I communication

From the perspective of cooperative V2I and V2V transmission, Liu et al. proposed an NC assisted scheduling scheme in [29] to enhance bandwidth efficiency and data dissemination performance in V2V/V2I cooperative networks. This approach involves three types of channels: one control channel and two service channels. The control channel is dedicated to disseminating management information and control messages, while the two service channels are used separately for broadcasting V2V and V2I messages. Consequently, V2V and V2I communication operate in an orthogonal manner, eliminating interference. Similarly, in [11], a collaborative V2V and V2I communication framework is utilized to offload computational tasks generated by vehicles within a vehicular edge computing network [30]. A joint task offloading and resource allocation scheme is proposed to minimize task processing latency. Specifically, tasks are profiled and prioritized based on parameters such as size, required computational resources, latency tolerance, and type, and are optimally offloaded to local nodes via V2V communication or to server nodes via V2I communication. Like [29], this work assumed orthogonal operation of V2V and V2I transmissions to avoid interference.

In contrast, several studies consider the co-channel interference between V2V and V2I transmissions due to spectrum reuse. For instance, Nguyen et al. [16] exploited cooperative V2V and V2I communication to provide uninterrupted service to passing vehicles. Assuming that V2V and V2I communication share the same service channels, a joint scheduling and power control scheme is proposed to optimize bandwidth allocation and maximize vehicle decoding probability. Further extending this work, the authors in [15] proposed a dynamic cooperative scheme for hybrid V2V/V2I networks. This scheme employs a dynamic forwarder selection strategy to establish adaptive multi-hop V2V paths, improving system throughput. Analytical results highlight the influence of RSU intervals, vehicle sharing preferences, and buffer capacity on connection continuity, service resumption time, and throughput. Similarly, Ref. [10] investigated V2V and V2I cooperation under spectrum reuse to enhance information dissemination and sustain vehicle service. The study evaluates throughput performance under additive white Gaussian noise (AWGN) and Rayleigh fading conditions, employing network coding to mitigate interference between V2V and V2I links. In another approach, Ref. [31] introduced a probabilistic opportunity channel access scheme (p-OCAS) to manage shared channels between V2V and V2I communication. By carefully selecting the access probability p, this scheme significantly reduces interference from RSUs on V2V communication while maintaining high RSU throughput. In scenarios such as post-disaster recovery, where communication infrastructures may be partially damaged, He et al. [20] explored cooperative V2V and V2I communication supported by air base stations (ABS) and non-orthogonal multiple access (NOMA) techniques. By optimizing spectrum reuse strategies, power control, and channel state information (CSI) latency, the system achieves improved energy efficiency while meeting reliability and rate requirements.

The aforementioned studies primarily focus on resource allocation for fixed V2V or V2I modes, overlooking the potential for vehicles to dynamically switch between these modes based on network topology, channel conditions, and vehicle preferences. Addressing this gap, Zhang et al. [32] proposed a trajectory-driven intelligent scheme to optimize V2V and V2I cooperation. This approach determines the mode of operation for vehicles and allocates bandwidth resources based on trajectory data, minimizing feedback overhead and maximizing utility functions related to data rates.

Despite the extensive research on cooperative V2V and V2I communication, several challenges remain. For instance, existing studies primarily emphasize connectivity while neglecting the nature of transmitted content and its impact on connectivity and reception performance. Moreover, the influence of SL feedback, supported since 3GPP Release 17, is often underestimated. Blind retransmission strategies in SL communication could incur significant feedback costs, warranting further investigation.

2.2 Network coding assisted data dissemination

From the perspective of NC, various techniques have been explored in the literature. Among these, RLNC is one of the most widely used methods to enhance reliability and throughput performance. For instance, in [33], Mosavat-Jahromi et al. proposed a distributed NC-based medium access control (NC-MAC) protocol for vehicular networks to improve the broadcast reliability of beacon information. In this approach, all bits in the transmitted content are treated with equal importance, which limits its effectiveness in applications such as scalable video dissemination.

To address the trade-off between coding cost and system throughput, Yang et al. [23] proposed a BATS coding scheme, building upon fountain and RLNC codes. In [24], BATS code is applied to cooperative V2I and V2V information-sharing networks to mitigate challenges posed by intermittent V2V/V2I links and lossy channel conditions. Specifically, during the V2I broadcast phase, the original content is encoded into batches using rateless fountain coding, with each batch comprising several encoded packets. In the subsequent V2V sharing phase, RLNC codes are generated from the encoded packets within the same batch and distributed to nearby vehicles. By carefully designing the BATS codes, the approach minimizes traffic overhead and total transmission delay. However, similar to RLNC, BATS coding does not provide UEP for video content dissemination, making it unsuitable for scenarios requiring prioritized delivery of video data.

From the above studies, it is evident that while RLNC does not require feedback and can generate coded packets akin to fountain codes, it struggles to address the diverse channel conditions of multiple users as it does not account for user states in its design. In contrast, ARNC generates coded packets while considering the current states of multiple receivers, which is achieved through frequent feedback from these receivers. However, this approach incurs significant feedback costs, posing a challenge in bandwidth-constrained environments.

In summary, there remains a pressing need for further research on the adaptive dissemination of video content in vehicular networks using cooperative V2V and V2I communication. Balancing the trade-off between received video quality and feedback costs is a key challenge in this domain. Motivated by this gap, we propose the PARNC-based scheduling scheme and optimize its associated parameters to maximize a formulated utility function that encapsulates the interplay between video quality and feedback costs.

3 System model

In this section, we elaborate the system model to study the video dissemination process in the NR V2X networks. Specifically, the network model of the cooperative V2V and V2I communication is firstly given, followed by the description of the transmission model. Then the ARNC and PARNC designs are stated, and the PARNC-based video dissemination scheduling scheme is also elaborated in this section.

3.1 Network model

As shown in Figure 1, we consider a bidirectional 4-lane straight road, and the width of each lane is w meters. The RSUs are sparsely deployed along the road, and the coverage radius and height of which are denoted by R and h, respectively. The considered road of interest is with $2D$ meters and an RSU is deployed at the midpoint of the considered road (with coordination $x = 0$). At time slot $t = 0$, we suppose there are N vehicles requesting a common location-based video content (such as HD map data) in each lane. The initial locations and moving speeds of the vehicles are randomly selected following uniform distributions from $-D$ to D and from $v_{\min}$ to $v_{\max}$, respectively. Due to the mobility, the locations of these vehicles are dynamic. Specifically, in slot t, the location of vehicle $I_{i,j}$ toward the midpoint of the considered road can be expressed as

$$r_{i,j}(t) = \begin{cases} r_{i,j}(0) + v_{i,j}t, \ i = 1, 2, \\ r_{i,j}(0) - v_{i,j}t, \ i = 3, 4. \end{cases} \tag{1}$$

In the formulation, i and j, respectively, denote the located lane of a particular vehicle and the corresponding index in the lane. Furthermore, we adopt a discrete-time system model where time is divided into slots, while the duration of a time-slot is small enough that the vehicle can be treated as quasi-static and $r_{i,j}$ is fixed in each particular time slot thereafter.

SVC technique is applied to encode the transmitted video data. Specifically, the original content is encoded into L layers of data, among which the first layer is called the BL and the other $(L-1)$ layers of data are called ELs. The BL contains the basic information of the encoded content, and can be successfully recovered with poor video quality. Additionally, the other $(L-1)$ ELs are used to gradually enhance the decoded video quality, but the decoding needs the help of all the lower layers because they cannot be decoded separately. Therefore, with SVC different vehicles can flexibly decode a particular number of video layers depending on the suffered channel condition and the video dissemination policy.

3.2 Transmission model

In the transmission process, we consider the cooperative V2I and V2V communication to combat the vehicles' mobility. For the V2I transmission, the RSU exploits the V2I multicast to disseminate the requested content to the vehicles. The V2I links are modeled using a Nakagami-m fading channel with parameter m_1 [34, 35]. This model is chosen for its flexibility and strong empirical basis in vehicular communication studies, as it can accurately represent a wide range of fading conditions by adjusting the m_1 parameter. Therefore, the received signal-to-noise ratio (SNR) at slot t, denoted by $\gamma^I_{i,j}(t)$, is expressed as

$$\gamma^I_{i,j}(t) = \frac{P_R g_{i,j} d^{-\alpha}_{i,j}(t)}{P_N}, \tag{2}$$

where i and j, respectively, denote the driving lane of the V2I vehicle and the identification number of the vehicle in the lane. P_R and P_N are the transmit powers of the RSU and noise, respectively. $d_{i,j}(t)$ is the distance between the RSU and vehicle $I_{i,j}$, and is expressed as

$$d_{i,j}(t) = \sqrt{h^2 + (i-1)^2 w^2 + r^2_{i,j}(t)}. \tag{3}$$

The channel gain $g_{i,j}$ of the considered Nakagami fading channel follows a gamma distribution with the expression that

$$f_g(x) = \left(\frac{m_1}{\Omega}\right)^{m_1} \frac{x^{m_1-1}}{\Gamma(m_1)} \exp\left(-\frac{m_1}{\Omega}x\right), \tag{4}$$

where $\Omega = \mathbf{E}(g)$ is the average power of g. Then, given the decoding threshold θ, the average successful transmission probability for a signal can be calculated as

$$p^I_{i,j}(t) = \mathbf{P}\left(\gamma^I_{i,j}(t) \geqslant \theta\right) = \frac{1}{\Gamma(m_1)} \Gamma\left(m_1, \frac{m_1}{\Omega} A(i,j,t)\right), \tag{5}$$

where $A(i,j,t) = \frac{\theta}{\alpha}\frac{P_N}{P_R}[d_{i,j}(t)]^{\alpha}$. In (5), $\Gamma(x)$ is the gamma function, and $\Gamma(z,x)$ denotes the upper incomplete gamma function. The derivation process of $p^I_{i,j}$ can be found in [24]. Similarly, for the V2V transmission, we also adopt the Nakagami-m fading model with parameter m_2 [34, 35]. This model, which is often characterized by rapid fluctuations and severe fading resilience, is particularly suitable for V2V scenarios. Thus, the successful transmission probability of V2V link can be expressed as

$$p^{V}_{i,j\to i',j'}(t)=\frac{1}{\Gamma\left(m_2\right)}\Gamma\left(m_2,\frac{m_2}{\Omega}B\left(i,j\to i',j',t\right)\right),\tag{6}$$

where $B(i,j\to i',j',t)=\frac{\theta}{\alpha}\frac{P_N}{P_V}\left[d_{i,j\to i',j'}\left(t\right)\right]^{\alpha}$, and P_V denotes the transmit power of a vehicle. In addition, the distance between the vehicle $I_{i,j}$ and $I_{i',j'}$ is calculated as

$$d_{i,j\to i',j'}\left(t\right)=\sqrt{\left(i-i'\right)^2w^2+\left[r_{i,j}\left(t\right)-r_{i',j'}\left(t\right)\right]^2}.\tag{7}$$

3.3 PARNC design

In the data dissemination, the NC technique is exploited to improve the transmission efficiency in the presence of multiple receivers and high mobility. The most commonly used NC technique is the RLNC, which is designed based on (8). Specifically, the RSU can continuously multicast RLNC packets that mix the total L layers of data up without the need of feedback from the receivers. Therefore, RLNC is a kind of blind retransmission scheme. s_{RLNC}, $\beta_{l,t}$ and x_l in (8), respectively, denote the transmitted packet, the NC coefficient for layer l of data in slot t, and the l-th layer of transmitted content. Each receiver successfully decodes the disseminated content if a sufficient number of RLNC packets are received, or gets nothing, otherwise.

$$s_{\mathrm{RLNC}}(t)=\sum_{l=1}^{L}\beta_{l,t}x_l.\tag{8}$$

For the ARNC, the RSU does not need to mix up all the L layers of data in one transmission. Instead, a generation parameter k is introduced and based on which the RSU generates an ARNC packet using the following formula:

$$s_{\mathrm{ARNC}}(t)=\sum_{l=1}^{k}\beta_{l,t}x_l.\tag{9}$$

This encoding scheme directly implements UEP. By controlling the generation parameter k, the transmitter controls the number of layers included in a packet. Crucially, the BL ($l=1$) is included in every transmitted packet (for any $k\geqslant 1$), ensuring it receives the highest level of protection against packet losses. ELs are included progressively; for example, layer $l=2$ is only included if $k\geqslant 2$, and layer $l=3$ only if $k\geqslant 3$. This creates a natural hierarchy where more important layers are transmitted more frequently, making them more resilient to channel errors. This inherent UEP property is a key advantage of ARNC over RLNC for scalable video multicast.

According to channel conditions and user preference, the RSU can adaptively determine the generation parameter k in each transmission. A vehicle n can decode the first l layers of data if the following criteria are met:

$$\begin{cases}\mathbb{1}\left[o\left(n,l\right)\right]\sum\limits_{j=1}^{l}\min\left(o\left(n,j\right),j\right)\geqslant l,\\ \sum\limits_{j=1}^{l+1}\min\left(o\left(n,j\right),j\right)<l+1,\end{cases}\tag{10}$$

where $\mathbb{1}(\cdot)$ is the indicator function, while $o(n,j)$ records the number of ARNC packets with generation j in the decoding process.

Figure 2 shows an example to illustrate the flexibility of ARNC under multiple receiver scenarios, and the performance of ARNC and RLNC for scalable video transmission is also compared. In the example, the original video is encoded into $L=4$ layers, the latency budget is assumed to be 4 time slots, and the generations are set to $k=2,4,1,4$, respectively. Two vehicles are involved in the data dissemination. Due to the interference and noise, the second and fourth transmissions to the vehicle 2 are failed, while all the four ARNC packets are successfully delivered to the vehicle 1. After four time slots, the vehicle 1 can successfully recover the $l=4$ layers of the disseminated video with high quality. Therefore, vehicle 2 receives two ARNC packets with $k=1$ and $k=2$, and the first two layers of the video content can be successfully decoded. In conclusion, by carefully designing the generation k different vehicles can adaptively receive the video layers complying with their suffered channel conditions. Also, UEP is illustrated in the ARNC design since no matter what generation is selected, the lowest layer is always involved, thus the lower layers of data are offered with more protection in the transmissions. Figure 2

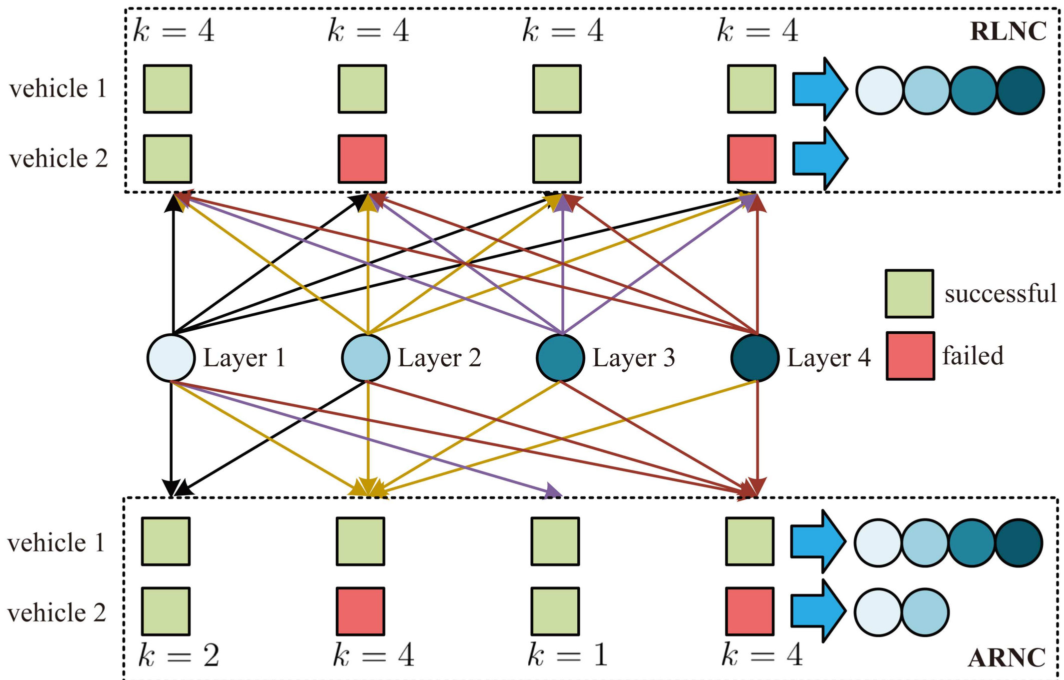

Figure 2 (Color online) Comparison of RLNC and ARNC.

also shows the performance of RLNC under the same situation as the ARNC. After four transmissions, the vehicle 1 can decode all the layers, but the vehicle 2 recovers nothing because insufficient RLNC packets are received, demonstrating the critical advantages of the UEP-enabled ARNC approach. In fact, the RLNC can be seen as a special kind of ARNC with $k = 4$.

From the comparison, we can observe that the ARNC performs better than the RLNC in the scalable video data dissemination, especially when the channel conditions of multiple users are diverse. The price of the performance superiority is the frequent feedback from receivers in ARNC, which means the vehicles need to send the transmission result back to the RSU, so that the RSU can update the network state and design the generation parameter k in the next transmission. We call such a scheme the full-feedback ARNC (FARNC) scheme for illustrative purposes. The frequent feedback may incur non-negligible signaling overhead, especially when the number of involved vehicles is huge.

To address the feedback overhead issue, we propose a novel scheme termed PARNC, which incorporates a tunable parameter p $(1 \leqslant p \leqslant T)$ to structure its operation into two consecutive phases, thereby striking an adaptive balance between transmission performance and feedback cost. In the first phase, spanning slots 1 to p, the RSU or V2V transmitter operates without any feedback from receivers. Throughout these initial transmissions, the generation parameter k is predefined in each slot t as $k = \min(t, L)$. This means that the first transmission contains only the BL ($k = 1$), the second includes both the BL and the first EL ($k = 2$), with subsequent transmissions following this pattern. This systematic approach ensures that the most critical video layers are disseminated first, providing a form of inherent UEP while completely eliminating feedback overhead during this phase. Beginning from slot $p+1$ until the deadline T, PARNC transitions to a second phase that operates analogously to conventional FARNC. In this phase, the transmitter collects feedback from receivers via the PSFCH to ascertain their current decoding states, and uses this information to adaptively determine the generation parameter k for each subsequent transmission. This allows the system to maximize the utility of each packet based on real-time network conditions. To further minimize feedback overhead, we assume that only successfully decoded packets trigger an ACK feedback; no feedback is sent in case of transmission failure or when a vehicle moves out of coverage.

The key advantage of PARNC lies in its hybrid structure. The initial feedback-free phase significantly reduces signaling overhead and saves valuable channel resources, which is especially beneficial in dense vehicular networks. At the same time, the UEP-oriented transmission strategy guarantees that all receivers can decode at least the BL, ensuring basic video quality regardless of channel variations. The subsequent feedback-assisted phase allows the system to recover most of the performance gap compared to the FARNC approach, thereby preserving the adaptive gains of network coding while operating under constrained feedback conditions. This makes PARNC particularly suitable for NR V2X networks where feedback resources are limited, yet high-quality video dissemination remains a priority.

3.4 PARNC-based scheduling scheme

In the data dissemination process, the vehicles retrieve content via V2V or V2I transmissions. Specifically, as shown in Figure 1, when the vehicles move into the RSU coverage, they turn to the V2I mode and receive the ARNC packets from the serving RSU. On the contrary, when vehicles travel outside of the RSU coverage, they will switch to V2V mode and retrieve or share contents with peer vehicles. To efficiently manage the V2V communication, in the system two V2V clusters are applied on the left and right sides of the RSU coverage, respectively. When a vehicle travels to the left side of the RSU coverage, it switches to the V2V mode, joins the V2V cluster 1 automatically, and retrieves the ARNC packets from the V2V transmitter (V2V Tx). Otherwise, if the vehicle dwells in the right side of the RSU coverage, it joins the V2V cluster 2 instead. The scheduling operation in the content dissemination is responsible for the following issues. First, the RSU needs to design the ARNC packets and select the most appropriate generation k for every V2I vehicle in the transmission. Second, for the V2V cluster 1 and cluster 2, the V2V Tx should be selected and the corresponding ARNC packets should be carefully designed. This is a challenging task since the scheduling decision maker needs to know the exact information of vehicles and their already received packets. Also, the selected V2V Tx also needs to know the topology of the involved V2V cluster. Due to the limited computing capacities of the vehicles and their energy-consuming concerns, it is not practical to rely on a vehicle performing complicated computing operations. Therefore, in the analysis, we prefer to study a simplified scheduling scheme. Specifically, the vehicle with the most decoding layers (denoted by $k_{\max}$) is selected as the V2V Tx, and $k_{\max}$ is chosen as the ARNC packet generation. This can significantly reduce the scheduling complexity of the vehicles and save the battery consumption. For V2I communication, the PARNC scheduling is applied, and the scheduling decision maker distributes the ARNC packets with predefined generations in the first p transmissions. After that the feedback from users is considered in the ARNC packet design like FARNC.

4 Problem formulation and solution

Based on the introduced system model and the PARNC-based scheduling scheme in Section 3.4, in this part we propose to formulate an optimization problem to evaluate the proposed PANRC scheme and the balance between the received quality and the feedback cost. Then a DRL algorithm is adopted to solve the formulated problem and achieve an efficient sub-optimal ARNC design.

4.1 Problem formulation

Suppose the deadline of the content dissemination is T time slots. With the introduced scheduling scheme, the vehicles can retrieve a particular number of ARNC packets from the serving RSU or V2V Tx. The feedback cost of the vehicle $I_{i,j}$, denoted by $\mathcal{U}_{i,j}^{f}$, can be presented as

$$\mathcal{U}_{i,j}^{f} = c_f n_{i,j}^{f}, \tag{11}$$

where c_f is the unit cost per feedback and $n_{i,j}^{f}$ is the number of feedbacks in the T transmissions. Also, with the number of decoded layers $k_{i,j}$, the transmission performance, i.e., the video-quality-related performance can be yielded as

$$\mathcal{U}_{i,j}^{t} = \begin{cases} \frac{1}{L}\sum\limits_{l=1}^{k_{i,j}} (L+1-l)\,, & k_{i,j} > 0, \\ 0, & k_{i,j} = 0. \end{cases} \tag{12}$$

We adopt such a formulation for two reasons. First, this is an increasing function regarding $k_{i,j}$. Therefore, the more layers are retrieved and then the higher transmission performance can be enjoyed by the vehicle. Second, with the growing number of layers in the received data packets, the marginal performance improvement from decoding one more layer gradually diminishes. This indicates the UEP feature in the video dissemination that the lower layers of the content are more important in the transmission.

Combining the transmission performance and feedback costs together, we can yield the following utility function to formulate the average performance of content dissemination with considering cooperative V2I and V2V communication:

$$\mathcal{U} = \frac{1}{N}\sum_{i,j}\left(\beta_t \mathcal{U}_{i,j}^{t} - \beta_f \mathcal{U}_{i,j}^{f}\right), \tag{13}$$

where β_t and β_f denote the coefficients of transmission performance and feedback costs, respectively. The utility function is mainly affected by the proposed scheduling scheme, especially the ARNC design of the serving RSU. If we define $\mathbf{\Pi} = \{a_1, a_2, \cdots, a_T\}$ as the applied scheduling scheme and a_t as the scheduling decision in slot t sampled under the scheme $\mathbf{\Pi}$, then we can get the following optimization problem:

$$\max_{\mathbf{\Pi}} \quad \mathcal{U} \tag{14}$$

$$\text{s.t.} \quad a_t = \min(t, L) \quad \text{if} \ \ t \leqslant p, \tag{15}$$

$$a_t \in [1, L] \quad \text{if} \ \ p < t \leqslant T. \tag{16}$$

In the formulation, the constraints (15) and (16) follow the design of PARNC which is elaborated in Section 3.3. By solving the problem, we can get the optimal scheduling decisions and code design of the proposed PARNC to maximize the average utility performance of the video dissemination.

4.2 Problem solution

In this subsection, our purpose is to obtain the optimal scheduling policy $\mathbf{\Pi}^*$ which can maximize the average utility values of all the vehicles after T transmissions, and $\mathbf{\Pi}^*$ is formulated in (14). This is a typical Markov decision process (MDP) problem, and DRL is one of the most commonly used solutions. Among all the available DRL algorithms, we employ the double deep Q network (DQN) to address the discrete action space and potential high dimensional state space which will be elaborated later [36].

The essence of Q learning is to carefully learn and update a Q table to present the scheduling policy $\mathbf{\Pi}$. To be specific, the Q table records the values of every particular state S and action a, indicating the value of the action a when the network is in state S. By learning and updating the parameters, the Q table can perfectly approximate the optimal scheduling policy $\mathbf{\Pi}$, and the best scheduling decision a_t can be sampled accordingly. However, the huge amount of state-action pairs makes it impossible to establish, maintain and train the whole Q table very well. Instead, we apply a deep neural network with parameters $\boldsymbol{w}$, i.e., $\boldsymbol{Q}(S, a|\boldsymbol{w})$, to approximate the Q table, and the optimal scheduling policy can be sampled by learning the parameters $\boldsymbol{w}$ and getting an optimal Q table. The pseudo-code of the introduced double DQN algorithm is shown in Algorithm 1. In the following we elaborate the working mechanism of the double DQN, but before that we need to determine the network state S, scheduling action a, and reward r used in the model.

Algorithm 1 Training process of the double DQN algorithm.

Input: Initial network state S_0; action space $\mathcal{A}$; step size α; decay factor γ; evaluation Q network Q with parameters $\boldsymbol{\omega}$; target Q network Q' with parameters $\boldsymbol{\omega'}$; mini-batch size m_{batch}; greedy epsilon ϵ; latency budget T; PARNC parameter p;
Output: Local optimal Q network parameters $\boldsymbol{\omega}^*$;

for iteration $= 1, 2, \cdots$ **do**
  Reset the network state S_0;
  for $t = 1, 2, \cdots, T$ **do**
    if $t \leqslant p$ **then**
      $a_t = \min(t, L)$;
    else
      Insert the network state S_t into the evaluation network Q, and sample the action a_t based on the ϵ-greedy strategy which is calculated in (18);
    end if
    Execute the action a_t to the environment, and observe the next state S_{t+1} as well as the corresponding reward r_t which is calculated in (17);
    Set the index $is\_end = 1$ if S_{t+1} is the terminal state, or $is\_end = 0$ otherwise;
    Store transition $(S_t, a_t, r_t, S_{t+1}, is\_end)$ in the ERB D;
    Randomly sample a mini-batch of m_{batch} transitions from D;
    Set

$$y_j = \begin{cases} r_j, & \text{if } is\_end = 1, \\ r_j + \gamma Q'\Big(S_{t+1}, \arg\max_{a'} Q\left(S_{t+1}, a'; \boldsymbol{\omega}\right); \boldsymbol{\omega'}\Big), & \text{if } is\_end = 0; \end{cases}$$

    Calculate the loss function

$$Loss = \frac{1}{m_{\text{batch}}} \sum_{j=1}^{m_{\text{batch}}} \left[y_j - Q\left(S_j, a_j; \boldsymbol{\omega}\right)\right]^2;$$

    Update the parameters $\boldsymbol{\omega}$ by performing a gradient descent on $\boldsymbol{\omega}$;
    Update $\boldsymbol{\omega'} := \boldsymbol{\omega}$ every C steps;
  end for
end for

• **Network state $\boldsymbol{S}$** represents the network parameters influencing the inference of scheduling decisions. Considering the feedback from vehicles, it is practical for the scheduling agent to know the received ARNC packets of vehicles, and sample the scheduling action based on the received packets. Therefore, the dimension of the network state $\boldsymbol{S}$ is $N \times L$, and $S(n,l)$ records the number of ARNC packets received by vehicle n with generation l.

• **Action $\boldsymbol{a}$** is sampled by the scheduling agent based on the maintained deep Q network and the current network state. All the potential $\boldsymbol{a}$'s form the action space $\mathcal{A} = \{1, 2, \cdots, L\}$. It should be mentioned that the V2V scheduling in the algorithm is simplified. Specifically, in each V2V cluster the vehicle that decodes the maximum number of layers (denoted as k_{max}) is selected as the V2V Tx. Notably, k_{max} corresponds to the designed ARNC generation parameter. For illustrative purposes, the V2V action is not presented in the DRL learning. Additionally, in the first p transmissions of every round, the action a_t is not sampled and is predefined as $\min(t, L)$ with $1 \leqslant t \leqslant p$ to comply with the constraints.

• **Reward $\boldsymbol{r}$** is the achieved immediate reward when the system is in state S and takes action a. In fact, the action not only impacts the performance in the current slot, but also has influence on the future scheduling actions as well as other vehicles. We use the following formulation to model the immediate reward r in time slot t:

$$r_t = \Delta\mathcal{U}(S_t, a_t) = \mathcal{U}(S_t, a_t) - \mathcal{U}(S_{t-1}, a_{t-1}), \tag{17}$$

where $\mathcal{U}(S_t, a_t)$ is given in (13).

At initialization, the algorithm randomly selects parameters for the evaluation network (EN) and the target network (TN). EN and TN have the same neural structures but different weight parameters, respectively, denoted by $\boldsymbol{w}$ and $\boldsymbol{w'}$. The EN is responsible to refer the action and update the Q table, while the TN is to mitigate the performance degradation caused by bootstrapping and overestimation. Except for the EN and TN, an experience replay buffer (ERB) is initialized, recording $(s, a, r, s\_, is\_end)$ vectors derived from the EN to update the parameters of EN and TN. $s\_$ in the ERB is the updated network state when the system takes the action a. Denote by D the capacity of the ERB, and the oldest record will be covered if the ERB is full and a new record is generated.

At slot $t = 0$, the locations of N vehicles are reset according to the system model, and every vehicle does not prefetch any content. The network state S is input to the EN and a scheduling action $\min(t, L)$ is generated complying with the behavior strategy. In this paper, the double DQN applies the following ϵ-greedy strategy:

$$a_t = \begin{cases} \arg\max\limits_{a} Q(S_t, a), & \text{with probability } 1-\epsilon, \\ \text{random selection}, & \text{with probability } \epsilon. \end{cases} \tag{18}$$

The strategy indicates that the network randomly selects an available action with probability ϵ or selects the a_t with the largest Q value otherwise. The probability ϵ guarantees the system can explore more potential actions so that the double DQN algorithm can avoid being stuck in the local optimum. After sufficient training and exploration, ϵ will degrade to a value near 0.

With the state S_0 and a_0, the RSU produces ARNC packets with generation a_0 and multicasts to the vehicles under its coverage. For the vehicles outside of the RSU coverage, they form different clusters and share RLNC packets with nearby peers as stated before. After transmission, the locations and held ARNC packets of every vehicle are updated, and the network state changes from S_0 to S_1 while the corresponding immediate reward r_0 can be calculated from (17) with $\mathcal{U}(S_{-1}, a_{-1}) \triangleq 0$. The vector $(S_0, a_0, r_0, S_1, is\_end)$ is stored in the ERB and then the next slot begins. The process continues T times and a round is finished, after which the network state is reset.

When the system runs enough rounds and sufficient samples are collected, the algorithm begins to update the EN and TN parameters. To be specific, the agent randomly selects a mini-batch of m_{batch} vectors to the ERB, and performs the following operations for every selected vector $(S_j, a_j, r_j, S_{j+1}, is\_end)$.

First of all, the EN and TN perform forward propagation, and respectively yield

$$q_j = Q(S_j, a_j|\boldsymbol{w}), \tag{19}$$

$$q_{j+1} = \max_{a_{j+1}} Q'(s_{j+1}, a_{j+1}|\boldsymbol{w'}). \tag{20}$$

Then the temporal difference (TD) target value y_j and the corresponding TD error can be calculated as

$$y_j = r_j + \gamma q_{j+1}, \tag{21}$$

$$\delta_j = q_j - y_j, \tag{22}$$

Table 1 Parameter setting.

Parameter	Value
Wide of a lane: w	4 m
Radius of the road: D	500 m
SNR threshold: θ	1
Power of AWGN noise: P_N	1×10^{-8} W
SVC layers : L	10
Latency budget: T	10 slots
Pathloss exponent: α	4
Number of vehicles: N	40
Coverage radius and height of RSU: (R, h)	(150, 4) m
Minimal and maximal speed: $[v_{\min}, v_{\max}]$	[11.2, 35] m/s
Transmit and feedback coefficient: $[\beta_t, \beta_f]$	[0.8, 0.2]
Transmit power of a RSU and vehicle: $[P_R, P_V]$	[1, 0.2] W

where γ is the decay coefficient, describing the influence of the current action on the future rewards. Then the agent performs the back propagation (BP) and yields the gradient $\nabla_{\boldsymbol{w}} Q(S_j, a_j|\boldsymbol{w})$, based on which the EN parameters $\boldsymbol{w}$ can be updated as

$$\boldsymbol{w} \leftarrow \boldsymbol{w} - \alpha\delta_j \nabla_{\boldsymbol{w}} Q(S_j, a_j|\boldsymbol{w}), \tag{23}$$

where α is the chosen learning rate and it is a hyperparameter. Also, the TN parameter $\boldsymbol{w'}$ is updated after every C steps,

$$\boldsymbol{w'} \leftarrow \tau \boldsymbol{w}. \tag{24}$$

5 Performance evaluation

In this section, we evaluate and compare the utility performance of different scheduling schemes under various network conditions using extensive simulations. We also investigate several interesting aspects, including the optimal selection of the probability parameter p under different scenarios. The parameters used in the simulations are summarized in Table 1. The road of interest is modeled as a $2D$ area with a length of $D = 1000$ m, and the width of each lane is set to $w = 4$ m. The coverage radius of the RSU is assumed to be $R = 150$ m, with a height of $h = 4$ m. The default number of vehicles is set to $N = 40$, with 10 vehicles per lane. The initial location of each vehicle is uniformly distributed within the range $[-D, D]$ m, and its driving velocity is randomly selected from the interval $[v_{\min}, v_{\max}] = [11.2, 35]$ m/s. For the transmission process, a Rayleigh fading channel is assumed for V2V and V2I communication, with the fading parameters $m_1 = m_2 = 1$ and a path loss factor of $\alpha = 4$. The decoding threshold for each transmitted packet is set to $\theta = 1$, and the noise power is defined as $P_N = 1 \times 10^{-8}$ W. The transmit power of the RSU and each vehicle is $P_R = 1$ W and $P_V = 0.2$ W, respectively. For the content and user preferences, we assume the disseminated video content is encoded into $L = 5$ layers. The latency budget for the transmission is set to $T = 10$ time slots, with each time slot corresponding to 1 s for the transmission of nonemergency large packets. In the simulations, we consider the following scheduling schemes to compare their performance under different scenarios.

- **FARNC [22, 26]:** At the beginning of each time slot, the RSU selects the ARNC packet depending on the current network state, and all the successful transmissions of V2I and V2V incur corresponding ACK feedback to update the network state.
- **PARNC:** In the first p ($p < T$) transmissions, the RSU chooses the predefined ARNC generation, i.e., $k = \min(t, L)$, and the feedback from the V2I transmissions is not needed. After the p transmissions, the RSU designs the ARNC packets in the same way as the FARNC. In the simulations, we set $p = 5$ by default.
- **No-feedback ARNC scheme (NARNC) [5]:** In the t-th transmission ($1 \leqslant t \leqslant T$), the ARNC generation from the RSU is predefined as $k = \min(t, L)$. NARNC is a special PARNC with $p = T$.
- **RLNC [37]:** In the t-th transmission ($1 \leqslant t \leqslant T$), the transmitted ARNC packet has generation of $k = L$.

Before conducting the detailed performance evaluations, we first examine the effect of the learning rate to ensure that the proposed double DQN model is properly trained and behaves as expected. Figure 3 shows the variation in the episode reward under four different learning rates. The results show that an excessively small learning rate (1×10^{-7}) leads to slow or low convergence, where the reward remains almost unchanged due to minimal parameter updates, whereas an overly large learning rate (0.1) causes pronounced oscillations and unstable learning. In

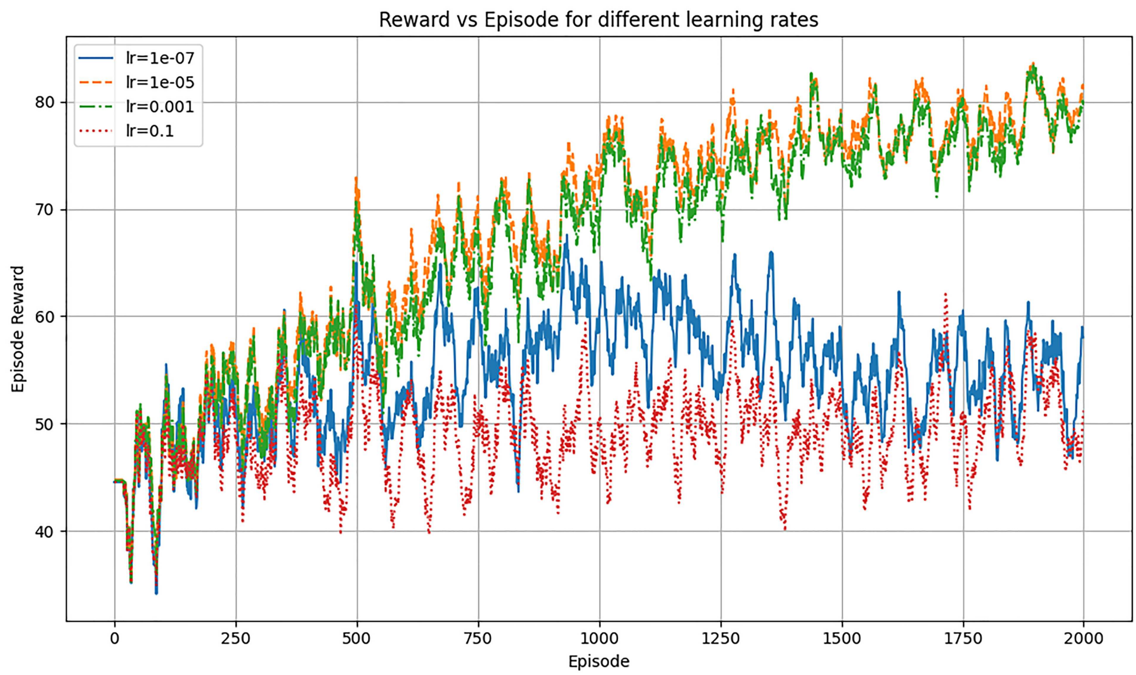

Figure 3 (Color online) Reward variation with training episodes under different learning rates. Moderate learning rates (1×10^{-5} and 1×10^{-3}) yield stable convergence, whereas too small (1×10^{-7}) or too large (0.1) rates result in poor performance.

contrast, moderate learning rates (1×10^{-5} and 1×10^{-3}) enable faster and more stable convergence with the highest rewards. These observations indicate that the proposed model exhibits normal learning behavior and achieves reliable convergence within a reasonable range of learning rates.

5.1 Impact of latency constraint T

In this subsection, we investigate and compare the utility performance of different scheduling schemes as the latency budget increases from 5 to 19 time slots. Figure 4(a) shows the utility performance of all the compared scheduling schemes in the scenario where the network prioritizes transmission utility, with parameters $\beta_f = 0.2$ and $\beta_t = 0.8$. From the figure, the following observations can be made.

First, the utility performance of all four scheduling schemes increases with the latency constraint T. This is intuitive, as a larger latency budget allows the RSU and V2V transmitters in each cluster to disseminate more network-coded packets, providing vehicles with a higher chance of receiving more video layers, which leads to an overall increase in utility performance.

When comparing the utility performance across different schemes, we observe that the proposed PARNC scheme outperforms the others, while the RLNC scheme achieves the worst performance. The FARNC and NARNC schemes fall between RLNC and PARNC. When $T < 8$ slots, NARNC performs better than FARNC, but beyond this threshold, FARNC achieves higher utility performance. These results show that PARNC is the best choice when transmission dominates the utility performance. When T is small, the network has limited opportunities to disseminate ARNC packets to vehicles, leading NARNC and FARNC to prioritize sending lower layers, resulting in comparable transmission performance for both schemes. Since FARNC requires frequent feedback, NARNC slightly outperforms FARNC in this range. As T increases, the RSU is required to transmit ARNC packets with $k = L$, but FARNC can still distribute packets with smaller k values, depending on network conditions. Due to user mobility and UEP, FARNC gradually outperforms NARNC as T increases.

Figure 4(b) shows the performance of the different schemes when the network prioritizes feedback cost, with $\beta_f = 0.8$ and $\beta_t = 0.2$. Several distinct observations emerge from this figure. For example, the FARNC scheme exhibits a decrease in utility, whereas NARNC shows a decreasing trend initially, followed by a gradual increase with T. This behavior can be explained as follows. When the feedback cost dominates the total utility, each received packet incurs a feedback cost. As the latency budget becomes more relaxed, the system generates more feedback from V2V and V2I dissemination, which increases the overall cost. The transmission utility is only realized after receiving the necessary packets, as defined by (10). Therefore, the FARNC scheme degrades as T increases. Although the NARNC scheme does not require feedback for V2I transmission, V2V transmissions still incur feedback

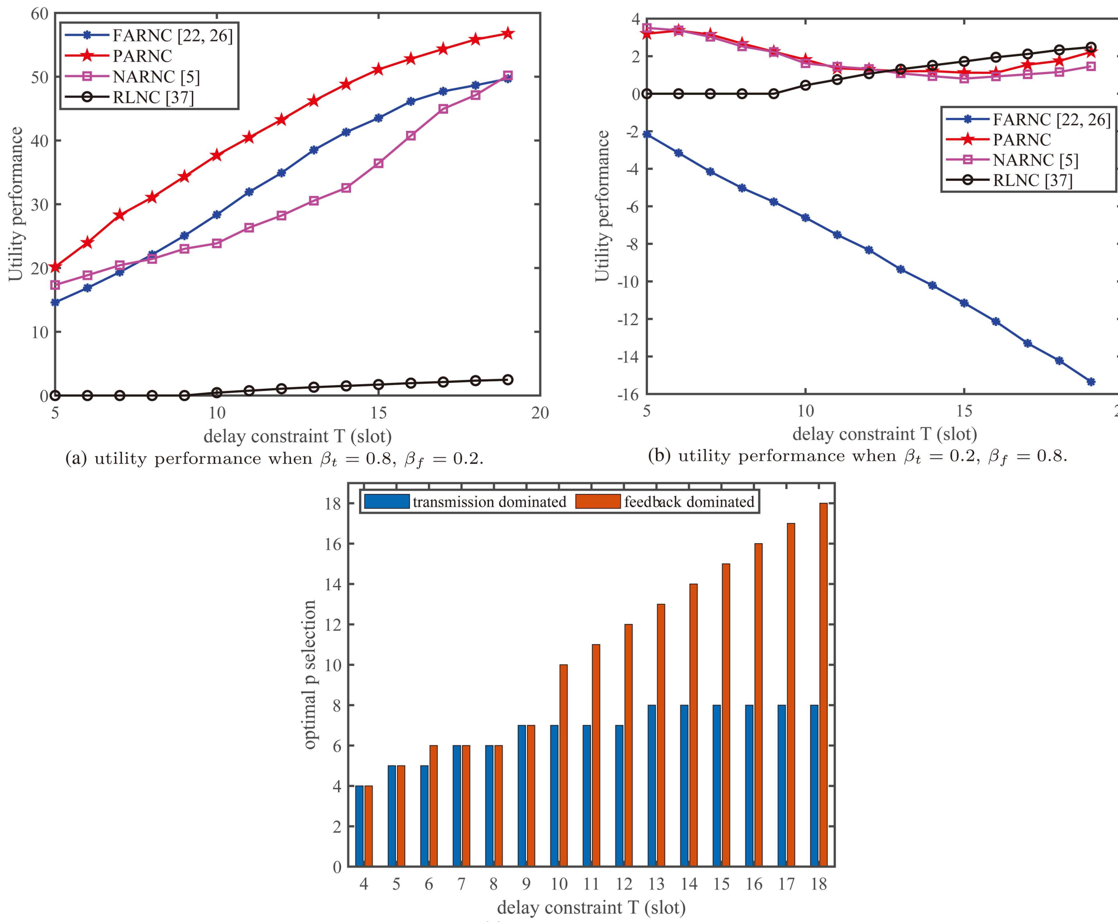

(a) utility performance when $\beta_t = 0.8$, $\beta_f = 0.2$.

(b) utility performance when $\beta_t = 0.2$, $\beta_f = 0.8$.

(c) best p selection.

Figure 4 (Color online) Utility performance comparison of different schemes under various latency budgets T's.

costs when vehicles decoding the initial layers of content enter a V2V cluster and are selected as V2V transmitters. As a result, the utility performance of NARNC initially decreases with T. However, as T increases, more vehicles can receive higher layers of content without additional feedback, leading to a slight increase in utility. Similarly, RLNC shows zero utility when $T < L$, as no vehicle can decode any content, but utility improves as more layers are decoded and no feedback costs are incurred. The proposed PARNC shows a performance trend similar to that of conventional NARNC, which is attributed to the two-phase design of PARNC. In the first phase ($t \leqslant p$), the ARNC operates with a generation parameter $k = \min(t, L)$ without relying on feedback information, thus incurring no feedback overhead. This design principle aligns with that of NARNC. In the second phase, the ARNC constructs its codewords in each time slot based on user feedback, which is consistent with traditional FARNC. When feedback overhead dominates the utility function, the PARNC scheme tends to mitigate the impact of feedback overhead on utility performance. As a result, the duration of the first phase is extended. As shown in Figure 4(c), the optimal p is essentially equal to T, meaning the first phase occupies all time slots without requiring feedback to guide the PARNC design. In this case, PARNC effectively degenerates into the NARNC scheme, leading to identical performance trends between the two schemes. Figure 4(b) shows that PARNC, NARNC and RLNC are suitable choices when the latency budget is either limited or relaxed, whereas the feedback-dependent scheme, like FARNC, performs poorly in these scenarios.

Given the flexibility of selecting various values for p in the PARNC scheme, we examine the performance of different p values under varying latency budgets and identify the optimal value of p (Figure 4(c)). The figure shows that the optimal p increases with T when transmission performance dominates the utility. In feedback-dominated scenarios, the optimal p satisfies $p = T$ for almost all T, meaning the optimal PARNC scheme converges to NARNC under these conditions, which is consistent with the findings from Figure 4(b).

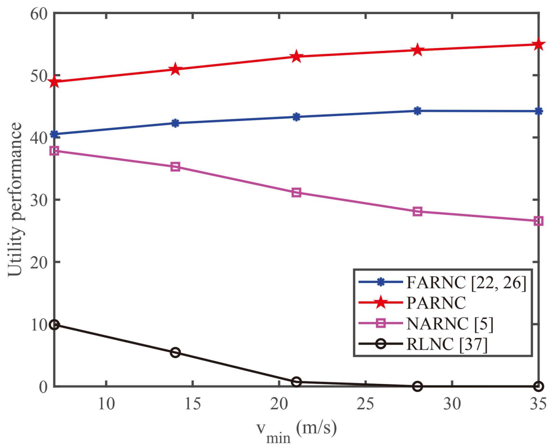

(a) utility performance when $\beta_t = 0.8$, $\beta_f = 0.2$.

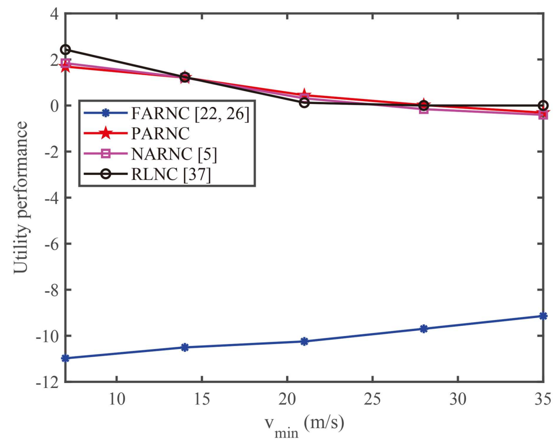

(b) utility performance when $\beta_t = 0.2$, $\beta_f = 0.8$.

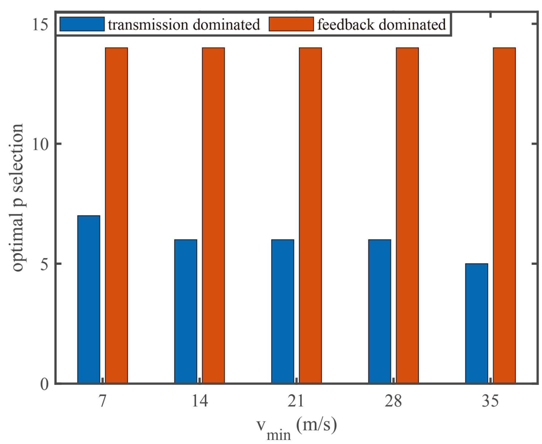

(c) best p selection.

Figure 5 (Color online) Utility performance comparison of different schemes under various lowest velocity $v_{\min}$'s.

5.2 Impact of vehicle mobility $v_{\min}$

In this subsection, we examine the impact of vehicle mobility on the final utility performance by varying the minimum velocity $v_{\min}$ from 7 to 35 m/s. A higher value of $v_{\min}$ indicates stronger vehicle mobility, leading to more frequent transitions between V2V/V2I and V2I/V2V modes. Since the FARNC and PARNC schemes are more flexible in designing ARNC packets and can exclusively disseminate packets involving lower layers of content (i.e., smaller values of k), the performance of these two schemes improves slightly as $v_{\min}$ increases (Figure 5(a)). This improvement is because FARNC and PARNC apply smaller values of k, making it more likely for V2I vehicles to decode the initial layers of content and then share them with surrounding V2V peers when they switch to V2V mode.

Although NARNC and RLNC may achieve higher transmission utility by including higher layers of content in the coded packets, higher mobility hinders vehicles from successfully decoding the disseminated packets or sharing them with others. As a result, the total utilities of both NARNC and RLNC decrease with increasing $v_{\min}$. Figure 5(c) shows a similar trend in the transmission-dominated scenario that the optimal value of p decreases as $v_{\min}$ increases. This suggests that when vehicle mobility is high, the RSU prefers to disseminate lower layers of content.

Additionally, in Figure 5(b), we compare the performance of different schemes under the system parameters $\beta_f = 0.8$ and $\beta_t = 0.2$. The results in this figure align with those observed in Figure 4(b), where the feedback-dependent FARNC scheme performs the worst, whereas the other feedback-independent schemes like PARNC, NARNC and RLNC perform similarly. The trend in Figure 5(c) under the feedback dominated scenario indicates that the optimal PARNC scheme degrades to NARNC as mobility increases, which complies with the results shown in Figure 5(b).

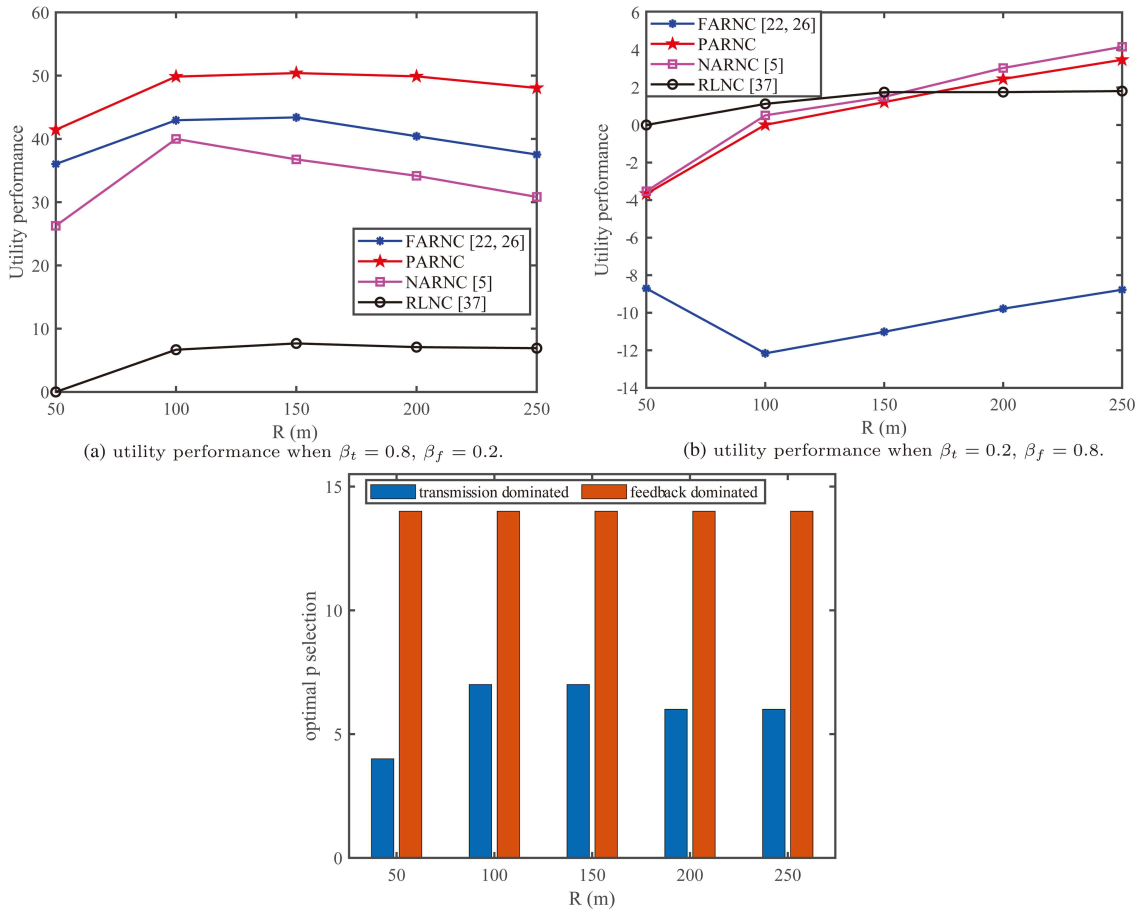

(a) utility performance when $\beta_t = 0.8$, $\beta_f = 0.2$.

(b) utility performance when $\beta_t = 0.2$, $\beta_f = 0.8$.

(c) best p selection.

Figure 6 (Color online) Utility performance comparison of different schemes under various RSU coverage R.

5.3 Impact of RSU coverage R

In this subsection, we analyze the impact of RSU coverage on the performance of different schemes by varying the coverage radius R from 50 to 250 m. Clearly, the value of R affects the mode selection of vehicles. Specifically, a larger R increases the likelihood that vehicles remain within RSU coverage and operate in the V2I mode, allowing them to receive more information from the RSU. In contrast, while vehicles in V2V mode can only share the layers they have already decoded, the ARNC design in the V2I mode is more flexible, improving transmission utility. However, if R becomes too large, the channel conditions between the RSU and the vehicle deteriorate, which may result in vehicles receiving little or no data from the RSU. In such cases, V2V transmission might be a better option for content retrieval.

As shown in Figure 6(a), the total utility of all the schemes initially increases with R and then begins to decrease slightly. This is because, at first, a larger R enhances the probability that vehicles can stay within the RSU coverage and receive more content. However, once R exceeds a certain threshold, the degradation in channel quality leads to diminishing returns in utility. From Figure 6(c), we observe that the optimal value of p increases with R under the transmission-dominated scenario, indicating that expanding RSU coverage positively impacts content dissemination and allows the RSU to transmit higher layers of data. When $R > 150$ m, the decrease in p reflects the fact that the RSU prefers to disseminate lower layers of content to mitigate the effects of deteriorating channel conditions, particularly for multiple vehicles. A comparison of the performance of different schemes in Figure 6(a) clearly shows the superiority of PARNC, with the performance gap between PARNC and FARNC widening as R increases.

Similarly, as shown in Figure 6(b), when $\beta_f = 0.8$ and $\beta_t = 0.2$, the growth of the utility function reaches a turning point, shifting from increasing to decreasing with R. This change is due to the increasing feedback costs, which make the feedback-dependent schemes less effective. As shown in Figure 6(c), the optimal PARNC scheme degrades to NARNC, which performs the best in this scenario, especially when R is large.

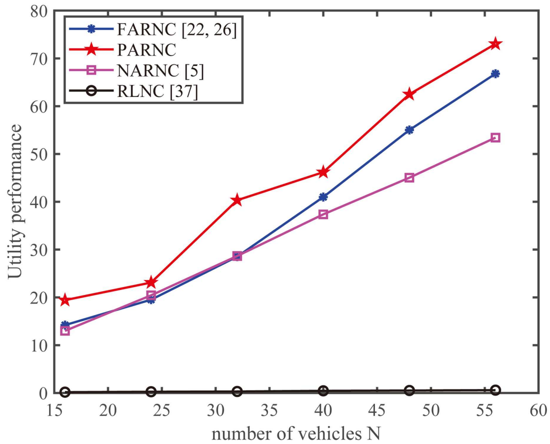

(a) utility performance when $\beta_t = 0.8$, $\beta_f = 0.2$.

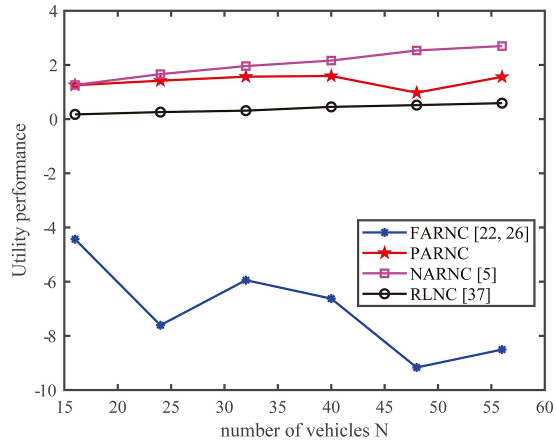

(b) utility performance when $\beta_t = 0.2$, $\beta_f = 0.8$.

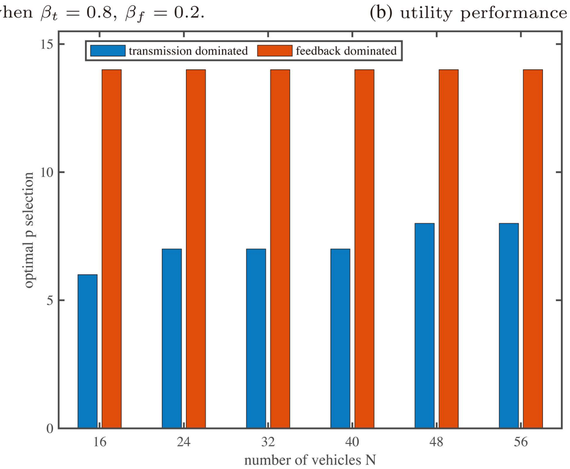

(c) best p selection.

Figure 7 (Color online) Utility performance comparison of different schemes under various vehicle numbers N.

5.4 Impact of number of vehicles N

In Figure 7, we study the utility performance of different schemes as the number of vehicles N increases. In fact, the increase in vehicle density may lead to the following effects. First, the total number of data packets transmitted and received in the system increases. As shown in Figure 7, the utility performance of most schemes improves with larger N. However, the FARNC scheme in Figure 7(b) is an exception whose performance decreases as N increases. This is because the system is more sensitive to feedback overhead under the parameter setting $\beta_f = 0.8$ and $\beta_t = 0.2$. Since each user may send feedback in every time slot in FARNC, the overall feedback cost increases significantly with the number of users, leading to a decline in utility performance. This can also be confirmed from Figure 7(c) that when the system prioritizes feedback cost, the optimal parameter p in the PARNC algorithm tends toward the total number of slots T, indicating a preference for operating without feedback.

An increase in vehicle number also complicates the transmission environment, leading to greater diversity in the combinations of packets received by users. This diversity raises the complexity of PARNC code design and challenges system performance optimization, potentially affecting the stability of the final utility function. Furthermore, experimental results indicate that the proposed PARNC scheme outperforms other compared schemes when $\beta_f = 0.2$, whereas PARNC performance approaches that of the optimal NARNC scheme when $\beta_f = 0.8$. The reasons for these phenomena have been discussed in Sections 5.1 and 5.2 and are not repeated here.

In summary, extensive simulations were conducted to compare the utility performance of the different scheduling schemes. The simulation results demonstrate that FARNC and RLNC are generally not suitable choices in cooperative V2V and V2I transmission-enabled vehicular networks. In cases where the network prioritizes transmission utility, PARNC outperforms all other schemes. However, when the feedback cost becomes dominant, the optimal PARNC scheme degrades to NARNC, which then provides superior performance compared to the other schemes.

6 Conclusion and future work

In this paper, we addressed the video content dissemination problem in NR V2X networks employing SL links, i.e., cooperative V2V and V2I transmissions. To enhance transmission efficiency and minimize feedback costs, we employed NC and SVC techniques and proposed a PARNC-based content scheduling scheme. We also introduced a utility function to evaluate the transmission performance and corresponding feedback costs, which are significantly influenced by the proposed scheduling scheme. Then, a DRL algorithm was applied to optimize the scheduling scheme and maximize the overall utility. Finally, extensive simulations were conducted to demonstrate the superiority of the proposed PARNC-based scheduling scheme across various scenarios, particularly when the transmission performance dominates the utility function and feedback costs are manageable.

Our analysis has identified several aspects that warrant further investigation, which we defer to future work. First, while the proposed PARNC scheme primarily addresses the tradeoff between transmission performance and feedback overhead, it does not consider decoding complexity. Thus, an ANRC scheme that balances decoding complexity and coding gain is required to reduce decoding latency. Second, although this study emphasizes the design and comparison of scheduling schemes, a thorough comparison of different DRL algorithms to determine optimal scheduling policies remains important. Further research is required to identify the most suitable DRL approach. Finally, this paper employs a simplified V2V cluster selection algorithm as an initial step. A more comprehensive and practical V2V transmitter selection mechanism should be developed to enhance the content dissemination efficiency of PARNC schemes.

Acknowledgements The work of Junchao MA was supported in part by National Natural Science Foundation of China (Grant No. 62401233), Natural Science Foundation of Jiangsu Province (Grant No. BK20241076), and 2023 Changzhou "Longcheng Talent Program" (Grant No. CQ20230073). The work of Pingzhi FAN was supported by National Natural Science Foundation of China (Grant No. 62020106001).

References

1 Garcia M H C, Molina-Galan A, Boban M, et al. A tutorial on 5G NR V2X communications. IEEE Commun Surv Tutorials, 2021, 23: 1972–2026
2 Chen S, Hu J, Shi Y, et al. Vehicle-to-everything (v2x) services supported by LTE-based systems and 5G. IEEE Comm Stand Mag, 2017, 1: 70–76
3 Chen S, Hu J, Zhao L, et al. Cellular Vehicle-to-Everything (C-V2X). Singapore: Springer Nature, 2023
4 Saad M M, Tariq M A, Seo J, et al. An overview of 3GPP release 17 & 18 advancements in the context of V2X technology. In: Proceedings of 2023 International Conference on Artificial Intelligence in Information and Communication (ICAIIC), 2023. 57–62
5 Akhtar A, Ma J, Shafn R, et al. Low latency scalable point cloud communication in VANETs using V2I communication. In: Proceedings of ICC 2019-2019 IEEE International Conference on Communications (ICC), 2019. 1–7
6 Min X K, Duan H Y, Sun W, et al. Perceptual video quality assessment: a survey. Sci China Inf Sci, 2024, 67: 211301
7 Ho I W H, Chau S C K, Magsino E R, et al. Efficient 3D road map data exchange for intelligent vehicles in vehicular fog networks. IEEE Trans Veh Technol, 2019, 69: 3151–3165
8 Harounabadi M, Soleymani D M, Bhadauria S, et al. V2X in 3GPP standardization: NR sidelink in release-16 and beyond. IEEE Comm Stand Mag, 2021, 5: 12–21
9 Bhatia J, Dave J, Bhavsar M, et al. SDN-enabled adaptive broadcast timer for data dissemination in vehicular ad hoc networks. IEEE Trans Veh Technol, 2021, 70: 8134–8147
10 Wang Q, Fan P, Letaief K B. On the joint V2I and V2V scheduling for cooperative VANETs with network coding. IEEE Trans Veh Technol, 2011, 61: 62–73
11 Fan W, Su Y, Liu J, et al. Joint task offloading and resource allocation for vehicular edge computing based on V2I and V2V modes. IEEE Trans Intell Transp Syst, 2023, 24: 4277–4292
12 Jiang X, Yu F R, Song T, et al. Resource allocation of video streaming over vehicular networks: a survey, some research issues and challenges. IEEE Trans Intell Transp Syst, 2022, 23: 5955–5975
13 Zhang X, Wei X, Zhou L, et al. Social-content-aware scalable video streaming in internet of video things. IEEE Internet Things J, 2021, 9: 830–843
14 Ma J, Liu L, Song H, et al. Scalable video transmission in cache-aided device-to-device networks. IEEE Trans Wireless Commun, 2020, 19: 4247–4261
15 Nguyen B L, Ngo D T, Tran N H, et al. Dynamic V2I/V2V cooperative scheme for connectivity and throughput enhancement. IEEE Trans Intell Transp Syst, 2020, 23: 1236–1246
16 Nguyen B L, Ngo D T, Dao M N, et al. A joint scheduling and power control scheme for hybrid I2V/V2V networks. IEEE Trans Veh Technol, 2020, 69: 15668–15681
17 Su L, Niu Y, Han Z, et al. Content distribution based on joint V2I and V2V scheduling in mmwave vehicular networks. IEEE Trans Veh Technol, 2022, 71: 3201–3213
18 Zhan W, Luo C, Wang J, et al. Deep-reinforcement-learning-based offloading scheduling for vehicular edge computing. IEEE Internet Things J, 2020, 7: 5449–5465
19 Häfner B, Bajpai V, Ott J, et al. A survey on cooperative architectures and maneuvers for connected and automated vehicles. IEEE Commun Surveys Tuts, 2022, 24: 380–403
20 He Y, Wang D, Huang F, et al. A V2I and V2V collaboration framework to support emergency communications in ABS-aided Internet of vehicles. IEEE Trans Green Commun Netw, 2023, 7: 2038–2051
21 Ahmed E, Gharavi H. Cooperative vehicular networking: a survey. IEEE Trans Intell Transp Syst, 2018, 19: 996–1014
22 Zhu F, Zhang C, Zheng Z, et al. Practical network coding technologies and softwarization in wireless networks. IEEE Internet Things J, 2021, 8: 5211–5218
23 Yang S, Yeung R W. Coding for a network coded fountain. In: Proceedings of 2011 IEEE International Symposium on Information Theory Proceedings, 2011. 2647–2651
24 Gao Y, Xu X, Guan Y L, et al. V2X content distribution based on batched network coding with distributed scheduling. IEEE Access, 2018, 6: 59449–59461
25 Ma J, Liu L, Song H, et al. On the fundamental tradeoffs between video freshness and video quality in real-time applications. IEEE Internet Things J, 2021, 8: 1492–1503

26 Li B, Li H, Li X, et al. Hybrid multicast and device-to-device communications based on adaptive random network coding. IEEE Trans Commun, 2019, 67: 2071–2083
27 Esmaeilzadeh M, Sadeghi P, Aboutorab N. Random linear network coding for wireless layered video broadcast: general design methods for adaptive feedback-free transmission. IEEE Trans Commun, 2017, 65: 790–805
28 Vukobratovic D, Stankovic V. Unequal error protection random linear coding strategies for erasure channels. IEEE Trans Commun, 2012, 60: 1243–1252
29 Liu K, Ng J K Y, Wang J, et al. Network-coding-assisted data dissemination via cooperative vehicle-to-vehicle/-infrastructure communications. IEEE Trans Intell Transp Syst, 2015, 17: 1509–1520
30 Shang B, Liu L, Tian Z. Deep learning-assisted energy-efficient task offloading in vehicular edge computing systems. IEEE Trans Veh Technol, 2021, 70: 9619–9624
31 Wen X, Chen J, Hu Z, et al. A p-opportunistic channel access scheme for interference mitigation between V2V and V2I communications. IEEE Internet Things J, 2020, 7: 3706–3718
32 Zhang Z, Li X, Liu D, et al. Trajectory data driven V2V/V2I mode switching and bandwidth allocation for vehicle networks. IEEE Wireless Commun. Lett., 2020, 9: 795–798
33 Mosavat-Jahromi H, Li Y, Cai L, et al. NC-MAC: a distributed MAC protocol for reliable beacon broadcasting in V2X. IEEE Trans Veh Technol, 2021, 70: 6044–6057
34 Rehman A, Di Marco P, Valentini R, et al. Performance analysis of intelligent reflecting surface-aided NR-V2X sidelink communications. In: Proceedings of 2024 IEEE 100th Vehicular Technology Conference (VTC2024-Fall), 2024. 1–6
35 Zhang G, Cao W, Gu X. Cooperative vehicular networks over Nakagami-m fading: joint power control and spectrum scheduling. Comput Netws, 2023, 237: 110052
36 van Hasselt H, Guez A, Silver D. Deep reinforcement learning with double Q-learning. In: Proceedings of the AAAI Conference on Artificial Intelligence, 2016. 2094–2100
37 Luo H, Wu Y, Sun G, et al. ESCM: an efficient and secure communication mechanism for UAV networks. IEEE Trans Netw Serv Manage, 2024, 21: 3124–3139